*P. Tadini, F. Maggi, L. T. DeLuca, *L. Anselmo, *C. Pardini,** M. Grassi, ***V. Trushlyakov.*
Politecnico di Milano, Milan, Italy
*ISTI/CNR, Pisa, Italy
**University of Naples "Federico II", Naples, Italy
***Omsk State Technical University, Omsk city, Russia

ACTIVE DEBRIS REMOVAL OF A COSMOS-3M SECOND STAGE BY HYBRID ROCKET MODULE

1. INTRODUCTION

The beginning of space exploration introduced a great number of objects on several orbits around the Earth. Each mission left something such as mechanical instruments, spacecraft components and upper rocket stages, that are all part of the famous category called *space junk*, or *space debris*. Moreover, when a spacecraft or a satellite comes to the end of its mission, it starts to be considered as a space debris. Over the last 40 years, the mass of the artificial objects in orbit increased quite steadily at the rate of about 145 metric tons annually, leading to a total tally of approximately 7000 metric tons[5]. Now, most of the cross-sectional area and mass is concentrated in about 4600 intact objects, i.e. abandoned spacecraft and rocket bodies, plus a further 1000 operational spacecraft. Simulations and parametric analyses have shown that the most efficient and effective way to prevent the outbreak of the "Kessler syndrome", i.e. the long-term exponential growth of the cataloged debris population, would be to remove enough cross-sectional area and mass from densely populated orbits. In practice, the active yearly removal of approximately 0.1% of the abandoned intact objects would be sufficient to stabilize the cataloged debris in Low Earth Orbit (LEO)[6], together with the worldwide adoption of the mitigation measures recommended by the IADC and the United Nations[2,3,4]. The IADC is an international governmental forum for the worldwide coordination of activities related to the issues of man-made and natural debris in space. Its primary purposes are to exchange information on space debris research activities between member space agencies, to facilitate opportunities for cooperation in space debris research, to review the progress of ongoing cooperative activities, and to identify debris mitigation options.

Since the 1980s, and in particular during the last 20 years, the effort of the international space community was concentrated on the worldwide adoption of mitigation measures, able to reduce or prevent the production of new orbital debris. Indeed in the last quarter of century, the progressive adoption of mitigation measures was quite successful in putting under control the growth of cataloged orbital debris produced by on-orbit accidental fragmentations, but the recent Chinese anti-satellite test (2007), which destroyed the old Fengyun 1C spacecraft in the most crowded circumterrestrial region[7], and the catastrophic accidental collision among Iridium 33 and Cosmos 2251 (2009), basically in the same LEO critical orbit range[8], led to the production of a huge amount of new cataloged fragments, putting the mitigation clock back twenty years. Moreover, as pointed out by Donald Kessler in the 1970s, and later on confirmed by several teams of researchers around the world with progressively more detailed long-term simulations of the orbital debris evolution around the Earth, the artificial objects with sizes of 10 cm or more, i.e. those "projectiles" able to cause the catastrophic fragmentation of a typical spacecraft or rocket body at the average collision velocity in LEO of 10 km/s, might continue to grow, in certain altitude ranges, even if drastic measures, such as an immediate and complete halt of launches and on-orbit explosions, were enforced[9,10,11,12,13]. In fact, the fragments of collisional events among the objects already in space might drive the evolution of the environment over several decades, resulting in an exponential increase of the cataloged fragments able to cause further catastrophic collisions. A collisional cascading ("Kessler syndrome") will finally follow, hampering any further space activity in certain altitude ranges[1,14,15]. For these reasons, it is being recognized that space debris mitigation alone might not be sufficient to guarantee the long-term utilization of some important orbital regimes. Considering the LEO regions, in particular the altitude ranges more prone to the "Kessler syndrome", the studies recently carried out indicated that the most efficient and effective way to contrast the ignition of a debris "chain reaction" would be remediation measures, that is the removal of a few large mass intact objects per year from the 3-5 most crowded altitude and inclination bands[6,11,12,13,16]. It was also shown that the removal of generic debris would lead to a growth reduction, but not to stabilization, because the reproduction of critical-size objects by collisions would more than balance the gain from removals[16].

Several innovative proposals for the active debris removal (ADR) are under development nowadays, with varying time frames of realization, however, most of them need in-orbit demonstration of reliability and applicability on a real mission. Concerning the choice of the propulsion system, a cost analysis for the de-orbiting of

a 1.2 metric ton IRS-1C satellite was presented for different propulsion options, suggesting that chemical rockets can be a viable solution[28]. Within this pool of technologies, solid propellants represent a simple, reliable and proven technology, even though characterized by low specific impulse and limited flexibility while liquid propellants fill the gaps left by the solids but larger volumes and higher degree of complexity are requested.

The capability of throttling and reignition may represent a stringent requirement for the adequate control of the final disposing maneuver, whereas a compact design is important for easier docking to the target and for dynamic stability of the final assembly (de-orbiting module and target). A compact volume may request a higher average propellant density, but may collide with ΔV requirements for a controlled reentry, needed by large systems. The thrust level should stem from a tradeoff choice between the risk of debris fragmentation and mission duration (correlated to propellant storability and collision risk during the maneuver). Considering this needs, hybrid rocket technology seems to be a valuable option for de-orbiting applications, due to the high specific impulse obtainable, intrinsic safety and, especially, thrust throttleability, possibility of green propellant and low cost technology[17,18]. Overall, a Hybrid Engine Module (HEM) represents a solution that mediates benefits and drawbacks from both liquid and solid technology. On one side, it presents throttleability and reignition capability typical of liquids, specific impulse levels which fall in between the performance of solid and liquid propulsion, and a higher mean propellant density due to the use of a solid fuel. However, a technological gap exists due to late development and lack of in-orbit demonstration.

The active debris removal by means of Hybrid Engine Modules aims at achieving contact and control of large abandoned objects, for example launcher vehicle's upper stages, which have then to be removed thanks to a dedicated de-orbiting kit.

2. Large Intact Object in LEO

Based on recent long-term simulation results[6,11,13,19], a broad consensus exists among the space debris experts: the targets of active removal are large intact objects in crowded regions of space, since they are a potential source of numerous debris posing a collision risk. The typical masses of the large targets for removal are between 500 and 1000 kg, in the case of spacecraft, and of more than 1000 kg, in the case of rocket upper stages. Generally the targets to be removed are ranked according to the following figure of merit: P_c (impact probability) $\times$ M (mass). However, the type of

orbit and the estimated lifetime – implicitly included in the estimation of the impact probability – should also be considered in planning active debris removal missions.

Presently (19 July 2012), following 4871 orbital launches, 3638 intact payloads and 1942 intact upper stages are in space, while 3452 satellites and 3603 rocket bodies have reentered in the atmosphere[20]. The current distribution of abandoned intact spacecraft and upper stages (Figure 1), together with the object ranking defined above[6], suggests that optimal active debris removal missions should be carried out in one of the following critical altitude (h) – inclination (i) bands:

1) h = 950 ± 100 km, i = 82° ± 1°;
2) h = 800 ± 100 km, i = 99° ± 1°;
3) h = 850 ± 100 km, i = 71° ± 1°;
4) h = 950 ± 100 km, i = 65° ± 1°;
5) h = 1000 ± 100 km, i = 74° ± 1°;
6) h = 750 ± 100 km, i = 74° ± 1°;
7) h = 600 ± 100 km, i = 82° ± 1°.

Taking into account the LEO distribution of intact objects (Figure 1) and the collision risk ranking[6], a very attractive target for active removal is represented by the Russian Cosmos-3M second stages, with mass of 1400 kg, diameter of 2.4 m and length of 6.5 m, of which 298 are in orbit as of 19 July 2012, mainly concentrated around two inclinations, 74° and 83° (Figure 2). In addition to their large number, they are significantly present in four critical altitude-inclination bands, i.e. the first (850-1050 km, i = 83°), the fourth (900-1050 km, i = 66°), the fifth (900-1000 km, i = 74°) and the sixth one (650-850 km, i = 74°).

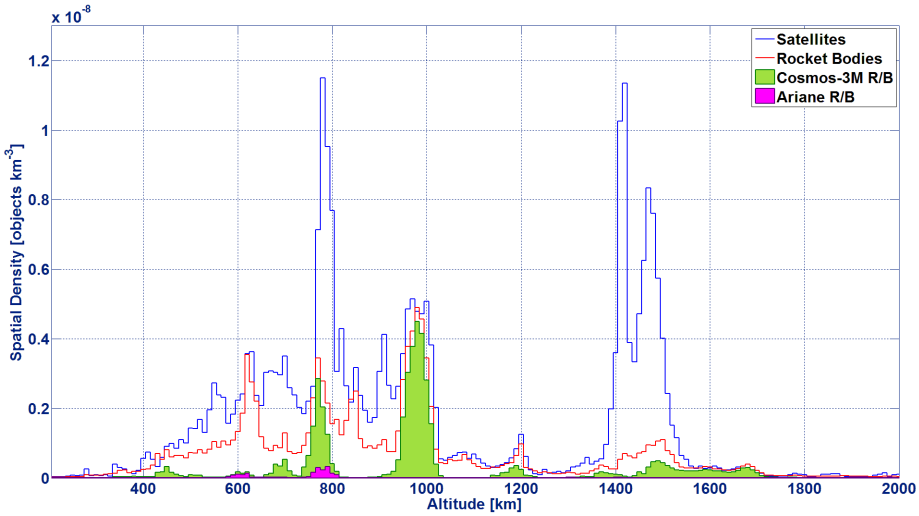

Figure 1 - Spatial density in LEO of intact satellites and rocket bodies (19 July 2012). The distribution of Cosmos-3M and Ariane upper stages is highlighted.

The targeting of this upper stage presents quite evident advantages: among them, the same capture techniques and procedures might be used many times over decades, it would be possible to operate in at least four separate altitude-inclination critical bands, the reentry risk assessment for de-orbiting (fragmentation analysis) should be carried out for only one object representative of the entire class, and the reduced set of de-orbiting kits needed might be tailored for small series production. In addition, multiple rendezvous might be possible within a single mission, because, for any given inclination, an average of about two stages would be present in each 5° bin of right ascension of the ascending node, with more favorable concentrations around specific orbit planes.

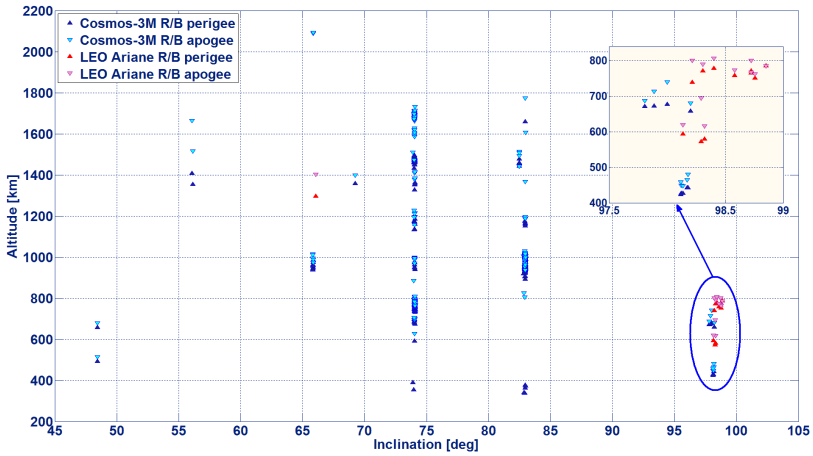

Figure 2 - Distribution of Ariane and Cosmos-3M rocket bodies (R/B) fully residing in LEO as a function of perigee/apogee altitude and inclination (19 July 2012).

Last, but not least, the choice of the Cosmos-3M second stages as targets for active debris removal would offer the occasion for a broad cooperation with Russia, concerning both the rocket body itself (Omsk State Technical University) and the eventual availability of launchers at low cost (Dnepr, Rokot) for the removal missions.

3. Mission

This study wants to remove an abandoned Cosmos-3M second stage from a critical orbit of 1000 km altitude, using a service platform made of the combination of several advanced technologies. An active debris removal mission involves many aspects:

- target rendezvous;
- capture and mating strategy;
- disposal strategy;
- controlled atmospheric reentry.

The service platform, or ADR platform, consists of a primary Hybrid Engine Module for the de-orbiting, a secondary propulsion system for rendezvous and attitude control, a docking system for the debris capture, as well as the avionics to manage the mission. It is assumed that the ADR platform should be injected in the same orbit plane of the target by the upper stage of a conventional space launcher, such as VEGA or Dnepr-1.

3.1 RENDEZVOUS STRATEGY

The rendezvous mission begins with the ADR platform already injected into the selected debris target orbit plane, in a lower altitude parking orbit. By exploiting the different orbital periods phasing with the target is achieved in order to start the rendezvous maneuver, which reduces to a few tens of kilometers the separation of the service platform from the Cosmos-3M stage expected location. This last one may have an error up to 1-2 km due to uncertainty in ground tracking and available Two-Line Elements (TLE) data set, which, as well known, are updated at prefixed time intervals[21]. Before starting far/mid-range rendezvous, the actual position of the debris target shall be determined by using optical sensors (and IR sensors to guarantee continuous coverage also during eclipse conditions) on board the service platform, such as a far range camera or a star sensor. Specifically, at this stage the most important information coming from the far range sensor is the bearing to the target, in order to correctly drive the approach maneuver. The range and range rate information can be also provided from the processing of the camera images. These information, together with the knowledge of the serving platform absolute orbit coming from a GPS receiver, allow determining the actual relative motion with respect to the target. Optical systems also allows a preliminary positive identification of the target as the one to be removed. Technology for far/mid range rendezvous should not represent a critical issue for the mission. Indeed, relevant hardware and methodologies could be inherited from already flown space missions, like Orbital Express[22] and the more recent PRISMA[23], which demonstrated in flight autonomous rendezvous and docking starting from distances up to a few hundreds of kilometers. Based on the relative position information, the ADR platform can be maneuvered to gradually approach the target. Specifically, the far/mid-range rendezvous maneuver has to bring the service platform to a close proximity of the target to start close-range rendezvous and then target capture (Figure 3).

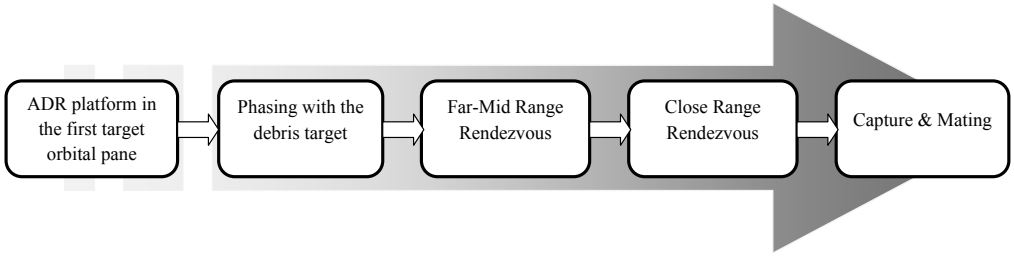

Figure 3 - Mission phases up to target capture.

When the separation from the target reduces to about a few meters, close range rendezvous is started with the relative position and attitude (pose) of the target determined by using laser ranging and optical cameras with monocular or stereo-vision techniques[24]. Close-proximity relative navigation poses significant technology challenges, since pose determination techniques for non-cooperating targets shall be implemented. Techniques and algorithms capable of extracting features of the target, such as binarization, contour mapping, and edge detection, could be used to set up the synthetic information that will be used to determine the relative pose[25,26,27]. Also in this case, although to a smaller extent, hardware and methodologies could be inherited from already flown rendezvous technology demonstration missions[22,23]. Before starting final approach for capture, a target fly around is performed for its final positive identification and inspection prior capture. This phase brings to the identification of the best points for capture, as well.

3.2 Debris Capture and Mating

The second stage of Cosmos-3M has a total length of 6.55 m and a diameter of 2.4 m. It is made up by two propellant tanks, that fill most of the volume, a liquid rocket engine (11D49) and payload connection structure on the frontal face. The engine has a total length of 1.78 m for an overall weight of 185 kg. The outflow area of the nozzle has a diameter of approximately 1.2 m, while the throat diameter is about 12 cm, with an area ratio of 103.4[41]. In order to remove a large object from its orbit, it is necessary to identify a point on its structure where connect the HEM. The second stage of Cosmos-3M offers three main points of connection:

- Lateral surface;
- Engine gas dynamic nozzle;
- Payload connection structure on the frontal face.

The structural part selected should be able to sustain very high stresses, due to the high thrusts generated by the chemical propulsion. Nevertheless a rocket stage is designed to withstand such kind of stress and high vibrations. The nozzle of the liquid rocket of the second stage of Cosmos-3M can be a possible docking point, due to its

high resistance to thermal, fluid dynamic and mechanical stresses. Assuming to have the possibility to approach the nozzle with an extremely accurate rendezvous maneuver, able to reduce significantly the relative velocity of the two objects, the HEM can insert a special titanium rod inside the nozzle to center the throat, using a group of micro-thrusters (RCS) to carry out this complicated maneuver. The HEM must lean against the divergent nozzle border where four clamps can hook it. At this point, placed on the top of the titanium rod, now completely inserted in the convergent part of the nozzle, a kind of corkscrew mechanism can be activated, performing the mating with the internal walls, by four titanium arms. The so called corkscrew system (Figure 4) is a threaded rod which moves four metal arms by cogwheels. This mechanism allows to enter through the throat diameter of 12 cm, thanks to the initial forward orientation of the arms, then, activated by electric actuators, it rotates back the four metal arms leaning against the internal convergent wall, involving a little compression of the nozzle, in order to keep it strictly connected to the HEM.

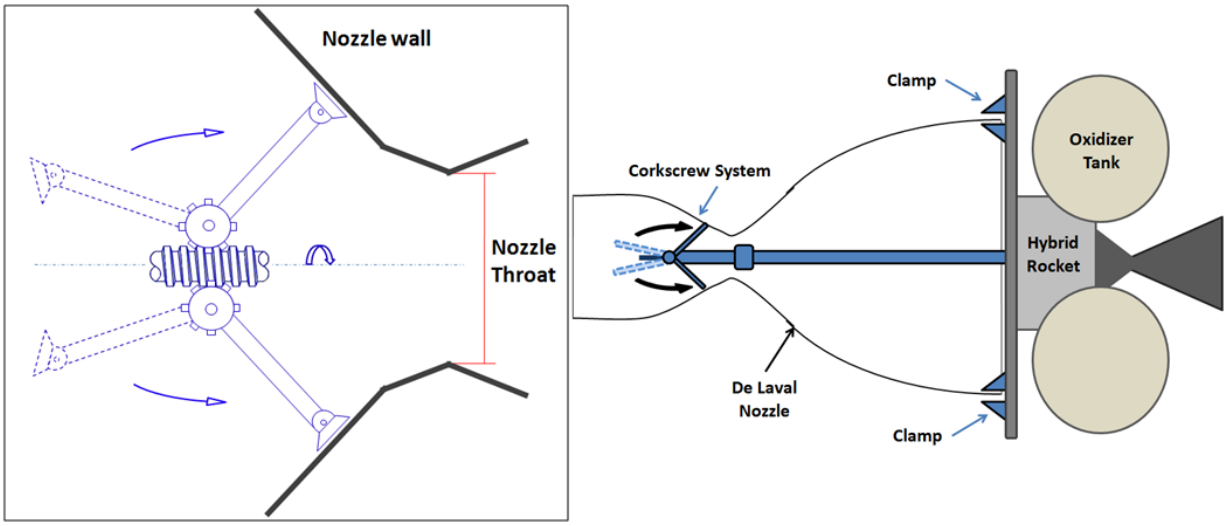

Figure 4 - Docking system for connection to the Cosmos-3M second stage nozzle. On the right the HEM position for the docking with the nozzle. On the left the detail of the mating mechanism.

Such kind of system could ensure the mating of the HEM with the Cosmos-3M nozzle and a sufficient stresses transmission during all maneuvers of the removal mission. However, this approach has to be investigated and tested.

3.3 Debris Disposal Strategy and Controlled Reentry

Having to return to the Earth a large object, such as a Cosmos-3M second stage, the de-orbiting mission must carry the debris from its original orbit down to an altitude where it is possible to direct it to a safe uninhabited oceanic area of the Earth, by a final impulse of thrust. In order to proceed with the preliminary sizing of the HEM, it

is possible to consider the transfer of the target from its position to a low parking orbit, with altitude around 250 km. After appropriate phasing on the parking orbit, a final impulse would decrease the perigee below the altitude of 100 km, from where the final reentry over the ocean, for example, will be guided (Figure 5).

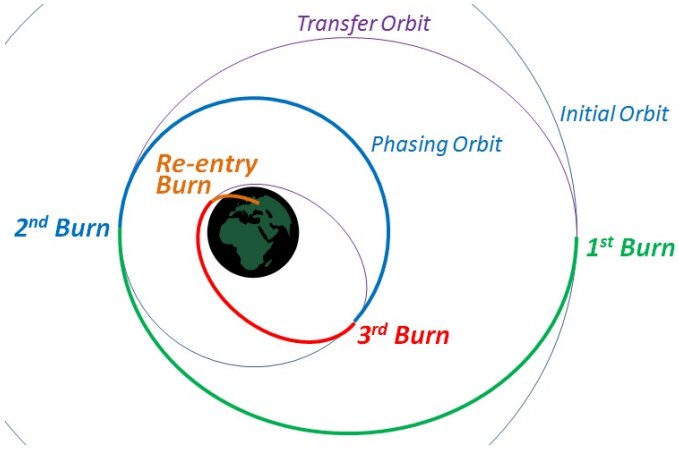

Figure 5 - Debris disposal strategy scheme.

For the purpose of this article, a Cosmos-3M second stage at an altitude of 1000 km is considered. By adopting a two body model for the transfer and a Hohmann maneuver, a Δv around 400 m/s is required to lower the orbit from 1000 km to 250 km. At this point, from this phasing orbit, there are two possibilities to carry out the object's atmospheric reentry. The cheapest, and easiest, method is to lower its perigee altitude in such a way that the atmospheric drag causes the object's orbit decay and, subsequently, its uncontrolled reentry. This is the typical disposal by orbit decay. The characteristic of this method consists in the impossibility to know a priori where the object will reach the Earth's surface. Even during the last orbits, it is very difficult to predict the exact location in which the reentry occurs, with a prediction uncertainty roughly 10% of the remaining lifetime[29]. This uncertainty must be considered in terms of reentry time, which means that an error of ten minutes is equivalent to approximately 5000 km of along-track uncertainty in the impact point of fragments. The alternative option is the disposal by controlled de-orbit, which provides more certainty in the impact location, sending the object in a safe area, such as the ocean or uninhabited lands, where the hazard to people and properties is minimized. This method is the most desirable when the debris is a large object, such as the second stage of Cosmos-3M, whose parts and components could survive, reaching the ground. Unfortunately the controlled disposal requires more propellant than the simple orbit decay. Indeed, in order to perform a controlled reentry of the Cosmos-3M second stage, from the phasing orbit of 250 km altitude, approximately 50 m/s are needed to lower the perigee to 90 km altitude, below the Karman line, then further

50 m/s should be considered for the final impulse to inject the debris into its descent trajectory through the atmosphere. This preliminary analysis provides a total velocity increment of 500 m/s, needed for the overall mission sizing.

Figure 6 - The controlled re-entry and subsequent breakup and fragmentation of the European Space Agency's "Jules Verne" Automated Transfer Vehicle (ATV)[30].

When an object begins the atmospheric reentry it is exposed to very strong heating and loads, thus the supporting structure starts to melt and release some pieces or internal components (Figure 6). This process of fragmentation goes on till the heating and load rates are low enough to prevent further disintegrations. The intensity of heating and load factor depends on the initial speed, the path flight angle and the ballistic coefficient of the falling object. The survivability of internal components depends on the shielding strength of the primary body and on their melting temperature. For what concern launcher upper stages, it is quite common that some components, such as tanks or combustion chamber, arrive almost intact to the ground, due to the high resistance to temperature of their materials.

Therefore, it is clear the importance of a controlled disposal for large objects such as abandoned launcher upper stages. The phasing orbit of 250 km should provide enough time to carry out the reentry maneuver in a safe way, following an optimized trajectory to reach any selected impact point on the Earth's surface.

4. HYBRID ENGINE MODULE (HEM)

A hybrid rocket engine typically features the oxidizer in the liquid or gaseous state, while the fuel is in the solid state. Its safety is guaranteed by no-contact between fuel and oxidizer, except during the combustion phase; after ignition, the two reactants give rise to a diffusion flame which develops within the boundary layer. Due to the type of flame, the rate of regression of solid grain is low, as well as thrust levels attainable, if compared with thrust provided by solid propulsion[31]. However the specific impulse obtainable by hybrid combustion is higher than solid propulsion, with the strong advantage of thrust throttleability, just by varying of oxidizer mass flow rate, and reignition,. These features give an high degree of flexibility, especially required by complex mission such as orbital transfers and controlled atmosphere

reentry. Furthermore hybrid technology offers the possibility to use green propellant and significant lower costs, than liquid propulsion. Hybrid rocket engines can also be built with a particular geometry, using a tangentially oxidizer injection, resulting very compact and highly efficient in combustion, thanks to the oxidizer flow that provides a vortex combustion. This particular kind of hybrid rocket engine results very small in size, if compared with classical long cylinder solid fuel shape. Such characteristics can be the right solution for space debris mitigation, by supplementing with this engine the new satellites that will reach space in the future. Moreover, this technology seems to be very promising even in the field of space debris remediation, making possible the active removal in LEO of large intact objects (up to several tonnes), by placing on their surface one Hybrid Engine Module, able to carry out all maneuvers required by an active removal debris mission.

4.1 Hybrid Rocket Combustion

In the simplest configuration, a hybrid rocket is made by a center-perforated solid fuel placed in the combustion chamber where an injector blows in a liquid or gaseous oxidizer. After the ignition the flame takes place within the turbulent boundary layer developed on the fuel surface, by the oxidizer flux. The flame is distributed between 10-20% of the boundary layer thickness. Inside a motor does not exist a free flux outside the boundary layer, since also the oxidizer passes through the central port of the solid fuel. Thus the flux behavior is more similar to that one developed in a pipe. It is affected by axial accelerations due to the enhancement of fuel mass flow rate (by pyrolysis) and combustion enthalpy as well as by the boundary layer thickness changes. Several studies, both empirical and theoretical, shows a strong reliance of fuel regression rate on the local mass flux along the solid fuel perforation[32]. The mathematical model which describes the regression rate behavior of classical hybrid is the *Heat-Transfer-Diffusion-Limited Theory* developed by Marxman et al. This theory has been confirmed by several following studies and modified to take into account the radiative heat exchange[32,33]. For practical applications, such as the sizing of an hybrid rocket, a more compact and simplified expression is used:

$$r_f = a_0 G_o^n \qquad [1]$$

where a_0, n are constant to evaluate experimentally. Typical n value for hybrid applications are between 0.4÷0.8. Eq. [1] is valid for an assigned solid fuel length[34]. The advantage of this expression is the dependence only on the specific oxidizer unitary mass flow rate G_o:

$$G_o = \frac{\dot{m}_o}{A_p} \qquad [2]$$

where A_p is the transversal area of the fuel central perforation. During combustion the regression rate value grows with the axial distance, thanks to the enhancement of mass flow rate, due to the addition of pyrolyzed fuel. On the contrary the increase of the central port area involves a regression rate decrease[32]. Sutton provides a r_f empirical correlation for the combustion of gaseous oxygen (GOX) and HTPB (hydroxyl-terminated polybutadiene), a polymer binder commonly used as solid fuel:

$$r_f = 0.03 G_o^{0.68} \quad [3]$$

with r_f in mm/s and G_o in kg/m^2·s. Eq. [3] was developed for a small-scale hybrid rocket[35], considering an oxidizer mass flow rate range of 35-280 kg/m^2·s. Unfortunately main disadvantage of the hybrid propulsion is the low value of fuel regression rate and its little sensibility to the variation of the operative conditions, as well the changing of mixture ratio O/F over time. Moreover the combustion is rather rough and inefficient, with efficiency around 95%, compared with solid (98%) and liquid propulsion (99%). Many solution to increase the fuel regression rate are under investigation, such as the addition of metal powders inside the polymeric fuel, in order to increase the heat exchange by radiation, or different kind of injection system and combustion chamber geometry, to optimize the heat exchange by convection. Other solutions consider the use of paraffin-based fuel, that show a very high regression rate but the mechanical properties of the solid grain are very low.

4.2 Non-classical Hybrid

Tests about non-classical hybrid started recently, from the mid-90s, with the objective to increase fuel regression rate in order to improve overall performance and design flexibility. Swirl oxidizer hybrid engine was experimented by Yuasa et al.[36,37], using a swirl injector located at the head end of the solid fuel, which has the classic cylindrical geometry. Several experiments, using PMMA as fuel and gaseous oxygen as oxidizer, showed an increase of fuel regression rate almost three times greater than that for traditional axial flow hybrid. The effect of the swirl strength does not interfere with the nature of the heat transfer in the turbulent flow, but improve its intensity. The increase of the swirl number provides a more uniform regression rate. Unfortunately the swirl intensity tends to decay fast over axial distance, decreasing its advantageous effects.

Knuth et al.[32] designed a totally new geometry for the combustion chamber with swirl injectors, able to generated a pair of coaxial, bidirection vortices in the combustion port. This configuration provides a fuel regression rate up to six times higher than a classic hybrid, for the couple gaseous oxygen and HTPB:

$$r_f = 0.193 G_o^{0.54} \quad [4]$$

The vortex hybrid shows a nearly neutral burn, suggested by the n value, thus a regression rate decrease over time is almost balanced by the increase of fuel surface area. While the mixture ratio and the mass burning rate remain nearly constant during combustion. In this kind of hybrid r_f seems to have a low dependence on G_{ox}, while a stronger dependence on injection velocities (more swirl strength) and fuel port geometry.

Haag et al.[38], at the Surrey Space Centre, have developed a particular vortex hybrid configuration called Vortex Flow Pancake (VFP), in which the oxidizer is injected tangentially in the combustion chamber, between two flat fuel disks (Figure 7). One disk regresses toward the engine face, the second one toward the nozzle backplate. In the center of the chamber diameter there is a central port, for the whole length of the chamber, that carry the hot gases to the nozzle. This vortex hybrid tested PMMA with gaseous oxygen, nitrous oxide and hydrogen peroxide. They observed strong influence of the oxidizer injection velocity on the fuel mass burning, which, on the contrary, was not affected by variation of the separation distance between the two fuel disks. Also the chamber pressure did not show significant effect on the combustion.

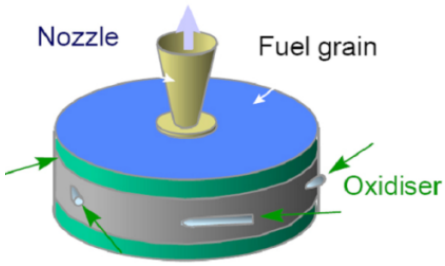

Figure 7 - Vortex Flow Pancake configuration, developed by Haag et al. at the end of 90s[38].

Rice et al. developed a similar configuration, but with a single fuel disk placed toward the motor face of the combustion chamber. They tested HTPB with gaseous oxygen, observing a significant sensitivity of fuel regression rate to injection velocity and separation distance, while significant effects by variation of chamber diameter[32]. They provide an empirical correlation for HTPB and GOX over the range tested, for low chamber pressures:

$$r_f = 0.40 G_o^{0.62} \quad [5]$$

This engine configuration is called Vortex End-Burning Hybrid (VEBH). Compared with classical hybrid, the regression rate with vortex combustion many times higher, or equal for lower value of G_o, that has a little meaning for geometries with fuel

disks. In conclusion vortex hybrid configurations promise to a very high design flexibility, for application that require compactness and short rocket lengths, such as upper stage propulsion system or active debris removal systems. However further tests are necessary to investigate the vortex behavior at high oxidizer mass flow rate, in the typical range of interest to classical hybrids for practical applications (500 $kg/m^2 \cdot s$), to verify also the possibility of scale predictably.

4.3 HEM FOR ACTIVE DEBRIS REMOVAL

For the development of the HEM, the attention is focused on HTPB (hydroxyl-terminated polybutadiene) and WAX as fuels, and N_2O or H_2O_2(90%) as oxidizers. This combinations of propellants provides vacuum specific impulses over 300 s and significant volumetric specific impulses, due to the high density of the oxidizers, especially for hydrogen peroxide (Figure 8). From the preliminary performance analysis done by means of CEA software (powered by NASA), it turns out that $I_{s\text{-}vac}$ values for HTPB and WAX are similar, with a slight advantage for the latter one while, in terms of I_v, HTPB performs better due to its higher density.

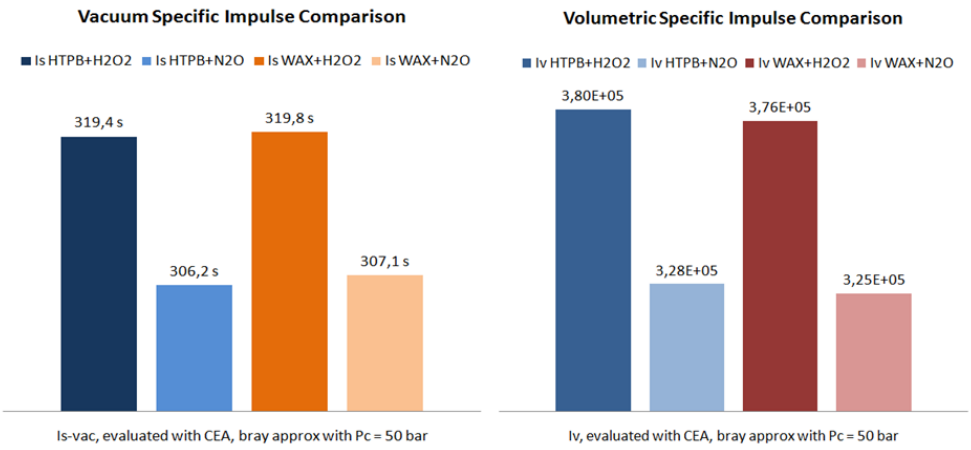

Figure 8 - Vacuum specific impulse and Volumetric Specific Impulse comparison between HTPB and WAX burning in H2O2 or N2O.

These results consider a Bray approximation referred to a nozzle expansion ratio of 100 and combustion chamber pressure of 50 bar. Turning to the choice of the oxidizer, catalytic decomposition hydrogen peroxide provides oxygen-rich 1000 K hot gases. Considering that ignition of HTPB solid fuel requires about 800 K, it is possible to develop a simple and reliable re-ignition system. Moreover, with a single tank of H_2O_2, it is possible to feed both the primary propulsion system and a set of RCS catalytic micro-thrusters. Though H_2O_2, with high concentration in water, is notorious for its storability issues, due to its decomposition inside tanks, but high level of peroxide purity and the use of appropriate materials have demonstrated that

risks can be avoided and the rate of dissociation can be reduced appreciably[40], allowing storability for space missions. Nevertheless low the main drawback of hybrid combustion process is regression rate, but different means are considered for the enhancement of mass burning rate spanning from the use of advanced additives to different injection approaches (vortex combustion and planar vortex pancake)[32,38,39]. These advanced designs of the combustion chamber, provides high combustion efficiency, low performance variation during combustion, and - in the case of solid metal additives - reduced emission of condensed combustion products (CCP), thanks to the vortex effect. All these improvements can provide smaller and very compact geometry, compared to classical hybrid, resulting very suitable to be attached to a large debris, such as Cosmos-3M second stage.

4.4 HEM Preliminary Sizing

In order to proceed with a preliminary design of a propulsion system is necessary to know the propulsion mission profile, in terms of vehicle velocity increments that, by Tsiolkovsky equation, are converted in a required amount of propellant mass:

$$\Delta v = g_0 I_s \ln\left(\frac{M_{initial}}{M_{final}}\right) \quad [6]$$

where g_0 is the gravity acceleration at sea level, I_s is the specific impulse provided by the motor while $M_{initial}$ and M_{final}, are the initial and final mass of the system, before and after the velocity increment. The initial mass contains the payload mass, the HEM mass, the mass of docking mechanism and the avionics. The payload mass for an active removal mission is the debris which, in this case, is the second stage of Cosmos-3M, having a weight of 1400 kg.

To calculate the mass of propellant $M_{prop} = M_{initial} - M_{final}$ is necessary to know an estimation value of I_s and the velocity increment required by the mission. The specific impulse estimation is provided by CEA software, which, for a fixed combination of fuel/oxidizer and a chosen value of nozzle area ratio, provides several performance parameters on varying the operative conditions in the combustion chamber, by calculating the chemical equilibrium product concentrations for the reactants couple. The total mission velocity increment depends on the type of maneuvers that the HEM must be able to carry out.

To de-orbit a second stage of Cosmos-3M are necessary four impulses of thrust:

- first and second impulse to perform the Hohmann transfer from an orbit of 1000 km to a phasing orbit of 250 km;
- a third impulse to lower the perigee from 250 km to 90 km of altitude;
- a fourth impulse to control the atmospheric reentry.

Knowing the equations that describe the Hohmann maneuver and common orbital maneuver, is possible to calculate the correspondent velocity increment for each impulse of thrust. For the considered mission we obtain:

- 1st impulse - Δv_{ell} = 199 m/s to get into a transfer elliptic orbit;
- 2nd impulse - Δv_{circ} = 204 m/s to get into the circular phasing orbit;
- 3rd impulse - Δv_{deo} = 48 m/s;
- 4th impulse - Δv_{ree} = 50 m/s.

For each impulse we considered a margin of 10%, obtaining a total velocity increment of 552 m/s. For the chosen propellant couple, HTPB + H_2O_2(90%), the thermo-chemical equilibrium calculation provides a vacuum specific impulse about 320 s. Now the last unknown is the HEM weight, which must be estimated by choosing an initial mass ratio between propellant and HEM:

$$K_{prop} = \frac{M_{prop}}{M_{HEM}} \qquad [7]$$

Now, considering an array with several HEM weight values and another one with different payload weights, is possible to draw a parametric graph which provides the HEM mass as function of payload weight, for a fixed value of velocity increment (Figure 9). At the first iteration it was consider a K_{prop} value equal to 0.7, kept from literature. Then after several iterations of the complete sizing algorithm, the K_{prop} estimated was around 0.6. In Figure 9, one can see many curves, corresponding to different debris altitude; the HEM weight value is already referred to the final K_{prop} calculated. Now is possible to use the estimation about the HEM to evaluate $M_{initial}$ and find, by inverting Eq. [6], M_{final}, hence the amount of propellant for the mission, M_{prop}. In the mass of the total system it was also considered an amount of around 40-50 kg to take into account the weight of avionics and docking system.

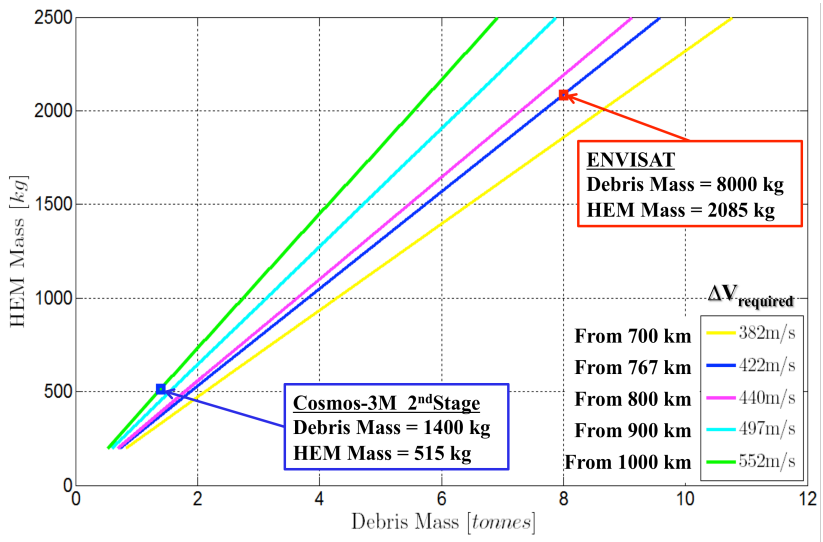

Figure 9 - HEM weight vs. Payload weight, for several values of velocity increment, corresponding to different debris altitudes. Inside the squares, two possible targets for ADR mission.

The total mass of propellant must be divided between all maneuvers. Then, by Tsiolkovsky equation, is possible to calculate the amount of propellant corresponding to each impulse of thrust, in particular, for a fixed value of mixture ratio O/F, selected for the preliminary performance estimation with CEA, we can find the relative portion of oxidizer and, consequently, the order of magnitude of oxidizer mass flow rate, $\dot{m}_o$. This data is essential to evaluate the regression rate r_f on varying the specific oxidizer mass flow rate, during the combustion. For a preliminary sizing it is consider a quasi-steady combustion and cylinder geometry for the solid fuel, HTPB, with a circular central perforation, typical hybrid configuration. Under the hypothesis of quasi-steady conditions it is supposed the slow variations of physical quantities inside the combustion chamber. This let to proceed with a preliminary size of the solid fuel geometry able to provide the defined propellant mass required by the mission.

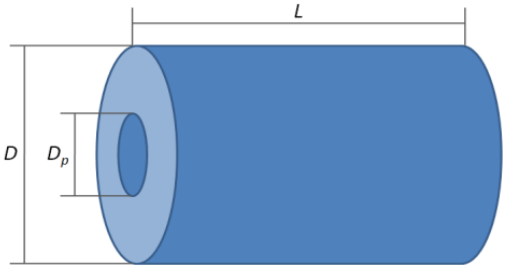

Figure 10 - Solid fuel geometry.

Considering the fuel regression rate correlation, by Sutton, for classical hybrid configuration:

$$r_f(t) = 0.03\left(\frac{4\dot{m}_o}{\pi D_p^2(t)}\right)^{0.68} \quad [8]$$

please note: for this mission we are considering the couple HTPB + H_2O_2(90%), but this correlation (Eq. [3]) is referred to the couple HTPB+GOX, since we do not have yet an empirical correlation for hydrogen peroxide. Nevertheless this is a preliminary analysis and the use of Eq.[3] is necessary to obtain an idea of possible performance and rocket sizing.

Starting from the initial value of perforation diameter, D_p, for a chosen dimension of the fuel geometry, and assuming to keep constant the oxidizer mass flow rate, is possible to calculate the corresponding G_o, so the fuel regression rate which let to obtain the instantaneous fuel burning rate:

$$\dot{m}_f(t) = \rho_f r_f(t) \pi L D_p(t) \quad [9]$$

where ρ_f is *HTPB* density and L the solid fuel length. Immediately is possible to calculate the mixture ratio O/F:

$$OF(t) = \dot{m}_o / \dot{m}_f(t) \quad [10]$$

and the propellant mass flow rate at the instant *t*:

$$\dot{m}_{prop}(t) = \dot{m}_o + \dot{m}_f(t) \quad [11]$$

The instantaneous pressure in the combustion chamber is equal to:

$$P_c(t) = \frac{c^*}{A_t} \dot{m}_{prop}(t) \quad [12]$$

where c^* is the characteristic velocity, a performance parameter provided by thermo-chemical calculation performed with CEA; it is a combustion efficiency indicator. While A_t is the throat area of the nozzle, sized on the maximum value of propellant mass flow rate. The following iteration will consider a new perforation diameter, due the solid fuel burned at the previous step. This iterative process proceeds forward as long as the propellant mass consumed meets the velocity increment required. Each iteration is equal to 1 s of combustion, so the iteration number corresponds to the combustion time. This algorithm is applied to each one of the four maneuver defined by the mission profile.

The same computation process is applied to an hybrid engine with vortex combustion. We choose the combustion chamber geometry of the Vortex Flow Pancake developed by Haag et al. and the fuel regression rate correlation evaluated by Rice et al. (it is referred to a very similar geometry, VEBH). In the case of vortex combustion the burning direction changes, because the solid fuel is made by two flat disks and the oxidizer is injected between them (Figure 7), generating a planar vortex which consumes the fuel along the disk height. Due to the definition of G_o, the vortex combustion can provide greater values of r_f than classic hybrid, for the same value of oxidizer mass flow rate.

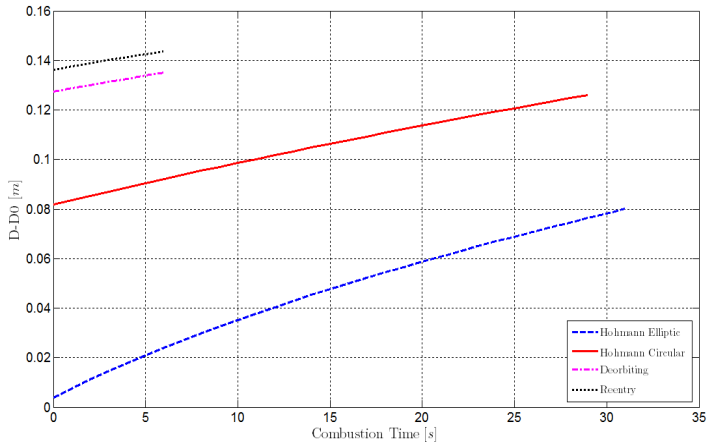

Figure 11 - D-D0 vs. combustion time, comparison between mission maneuvers.

In Figure 11, one can see the change of solid fuel instantaneous diameter, normalized on initial perforation diameter, over time of combustion. The two impulses of Hohmann maneuver are the most expensive of the mission, to reach about 200 m/s of velocity increment are necessary almost 30 s. While the last orbit transfer and the final impulse to perform the atmospheric reentry require six seconds of combustion.

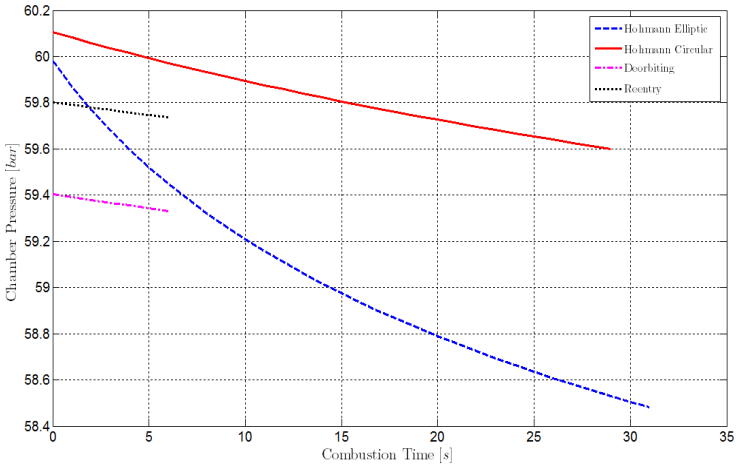

Figure 12 - Combustion Pressure vs. Time, comparison between mission maneuvers.

The chamber pressure ranges between 59 and 60 bar, quite constant during combustion, without significant variation. The initial oxidizer mass flow rate value was chosen to generate a combustion pressure of 60 bar, for each maneuver, according to the preliminary performance evaluation performed with CEA.

By the knowledge of the trend of physical quantities during the combustion, is possible to obtain all performance parameters, such as the thrust and the specific impulse over combustion time. The calculation considers losses, due to the divergent angle of the conic nozzle and the positive contribute given by gas dynamic expansion in the vacuum. The thrust is generated by a conic nozzle, with an high angle of divergent to keep a short nozzle length to the detriment of performance. The best solution is a bell nozzle, shorter than conic, and optimized for the hot gases expansion.

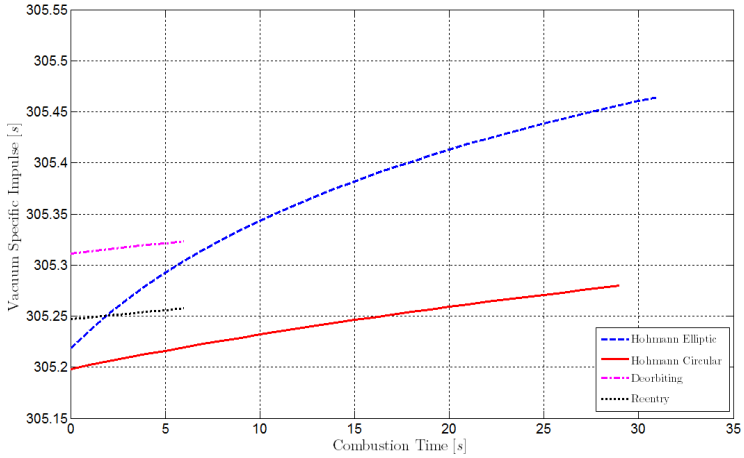

Figure 13 - Vacuum Specific Impulse vs. Combustion Time, comparison between mission maneuvers.

The specific impulse resulted is equal to 305 s, less than the initial estimation but enough to meet the requirements of mission. One can see that it remains quite constant during combustion time for all maneuvers (Figure 13). The HEM can provide about 12 kN of thrust, subjecting the second stage of Cosmos-3M, therefore the mating system, to accelerations below 1g (Figure 14).

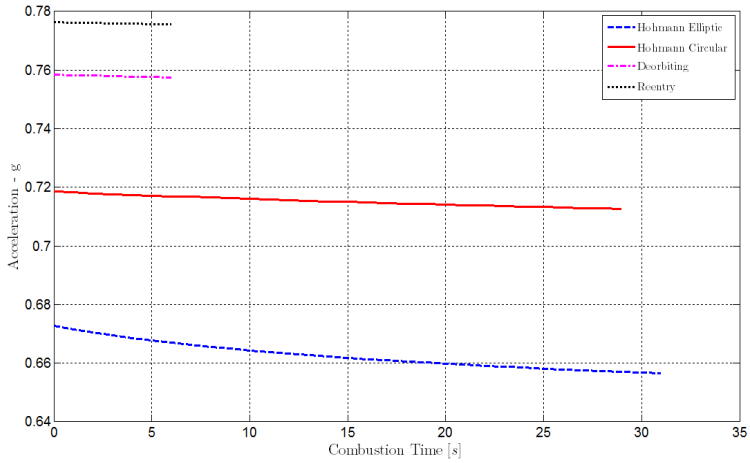

Figure 14 - Acceleration vs. Combustion Time, comparison between mission maneuvers.

Once evaluated the rocket performance, is possible to proceed with the sizing of all engine components:

- *Combustion chamber:* made by titanium, due to its high mechanical properties and low density;
- *Nozzle:* conical convergent and divergent made by pyrolitic graphite, commonly used for rocket nozzles;
- *Tanks:* four spherical tanks made by aluminum, which, with its low density, allows to keep a low weight. The pressurization is made by a membrane

directly inside each tank, solution often chosen by Russians. The pressurization gas is N_2.

- *Ignition system:* catalytic bed made by aluminum oxide, which is able to activate the hydrogen peroxide decomposition, generating hot gases with temperature about 1000 K. This allows the use of steel for the catalytic chamber and pipe, reducing costs;
- *Pipe and Valves:* for these components we considered a weight corresponding to the 20% of the combustion chamber dry weight;
- *Connection Structure:* it is not still designed a structure to connect all engine components with the docking system and the avionics. Thus, we take into account an amount of weight or about 30-35 kg.

In addition, it was sized an attitude control system (RCS) made up by twelve catalytic micro-thrusters. We estimated the magnitude of a single impulse of thrust and a minimum number of impulses to control each maneuver. In order to take into account the corresponding further amount of oxidizer for the tanks sizing, as well the weight of all micro-thrusters.

The sizing provides the HEM total weight and the ratio K_p, between propellant and HEM mass. If the engine obtained fulfills the performance requirements for each maneuver, this will be the final mass for per preliminary sizing of the Hybrid Engine Module for the active debris removal mission of the second stage of Cosmos-3M. Otherwise it is necessary to perform a new complete iteration modifying the initial solid fuel dimensions.

4.5 HEM SIZE

For what concern the classic hybrid, the combustion chamber results to have an external diameter of 25 cm, while the total rocket length, including the nozzle, is of 176 cm (Figure 15). The solid fuel, inside the chamber, is 100 cm long with a radius of about 12 cm. The length of the combustion chamber takes into account the presence of a pre and post chamber, essential for the flame attachment on the solid fuel and for a better mixing of hot gases generated. Each tank has an external diameter of 58 cm. The total HEM weight, considering all the propellant loaded, is about 513 kg. The propellant mass is 320 kg, 35 kg of HTPB and about 284 kg of hydrogen peroxide. Considering to place the four tanks on the rocket side, the diameter of the total system is 144 cm.

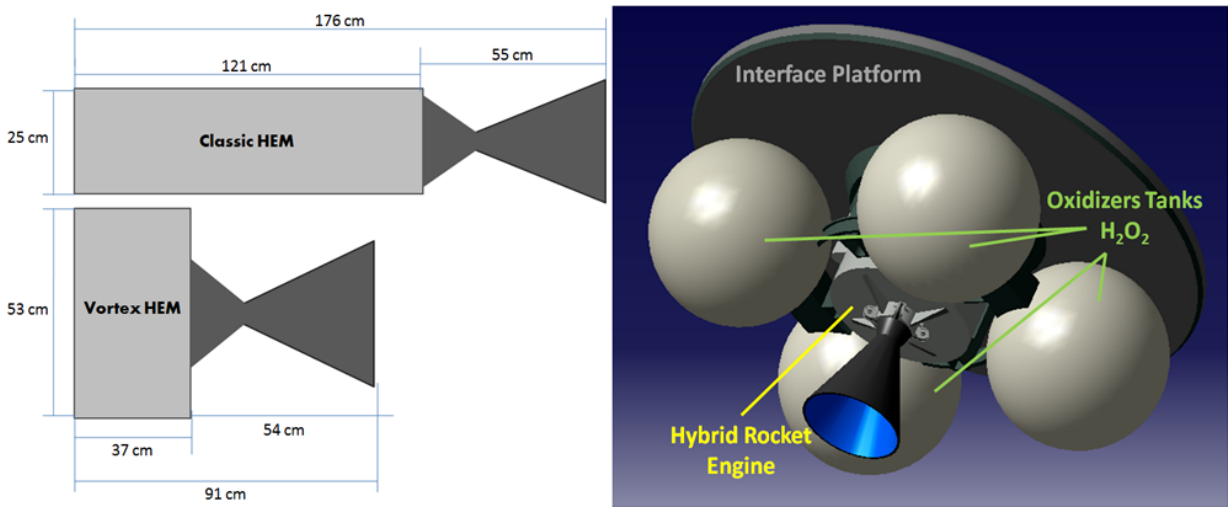

Figure 15- Size comparison between Classical and Vortex HEM (left). HEM conceptual sketch for Vortex Flow Pancake configuration (right).

Concerning the vortex hybrid (VFP), the combustion chamber results with an external diameter of 53 cm, while the total rocket length, including the nozzle, is of 91 cm. The solid fuel disk is 20 cm height with a radius of about 25 cm. Each tank has an external diameter of 57 cm. The total HEM weight, considering all the propellant loaded, is about 534 kg. The propellant mass is 320 kg, 54 kg of HTPB and about 266 kg of hydrogen peroxide. Considering to place the four tanks on the rocket side (Figure 15), the diameter of the total system is 170 cm.

5. CONCLUSIONS

The active debris removal of a large object, such as the second stage of Cosmos-3M, is a complex mission which requires the combination of several advanced technologies. A very crucial aspect is the selection of propulsion system, since it must allow the safe removing of the target from a LEO orbit and its controlled reentry in the atmosphere. Hybrid rocket technology seems to be a valuable option due to its high performance and flexible functioning. In particular the use of hydrogen peroxide as oxidizer, provides several advantages: high density, high performance with HTPB and easy reignition capability, monopropellant for attitude control system (RCS). From the preliminary sizing of the Hybrid Engine Module results a propulsion system with a wet weight of approximately 520 kg, a specific impulse of 305 s and thrusts of the order of 12-15 kN. Several tests on non-classical hybrid engines have demonstrated the possibility to obtain higher combustion efficiency and performance than typical hybrid rockets, keeping, in addition, very compact sizes. Nevertheless the hybrid vortex combustion has still to be tested at high ranges of specific oxidizer mass flow rate, typically classic hybrid operative conditions. For the considered mission the diameter of a VFP hybrid engine results of 53 cm, with a total engine

length of 91 cm (including nozzle). Such little dimensions make easier the realization of a full-scale engine demonstrator, starting from lab-scale experimental tests, thanks to the small jump of scale. The resulting sizes of HEM as well its weight allow to use low-cost space launchers, such as VEGA or Dnepr-1 and, considering the total launcher carrying capacity (for example VEGA carries about 1500 kg to LEO), multiple ADR missions can be performed by a single launch.

REFERENCES

1. Kessler, D.J., Cour-Palais, B.G. Collision frequency of artificial satellites: Creation of a debris belt, *Journal of Geophysical Research*, 83 (1978) 2637-2646.
2. IADC Steering Group & Working Group 4. Space debris mitigation guidelines, IADC-02-01, Inter-Agency Space Debris Coordination Committee (IADC), 2002.
3. UNCOPUOS. Space debris mitigation guidelines of the United Nations Committee on the Peaceful Uses of Outer Space, A/62/20 (2007), Endorsed by the General Assembly Resolution A/RES/62/217, United Nations, New York, USA, 2008.
4. IADC Steering Group & Working Group 4. Space debris mitigation guidelines. IADC-02-01, rev. 1, Inter-Agency Space Debris Coordination Committee (IADC), 2007.
5. IADC Steering Group. Space debris: IADC assessment report for 2010, Inter-Agency Space Debris Coordination Committee (IADC), 2012.
6. Liou, J.-C. An active debris removal parametric study for LEO environment remediation, *Advances in Space Research*, 47 (2011) 1865-1876.
7. Pardini C., Anselmo L. Assessment of the consequences of the Fengyun-1C breakup in low Earth orbit, *Advances in Space Research*, 44 (2009) 545-557.
8. Pardini C., Anselmo L. Physical properties and long-term evolution of the debris clouds produced by two catastrophic collisions in Earth orbit, *Advances in Space Research*, 48 (2011) 557-569.
9. Rossi, A., Anselmo, L., Pardini, C., Valsecchi, G.B. Analysis of mitigation measures based on the Semi-Deterministic Model. Final Report of ESA/ESOC Contract No. 18423/04/D/HK, Version 3.0, ISTI-CNR, Pisa, Italy, 2009.
10. Rossi, A., Anselmo, L., Pardini, C., Valsecchi, G.B., Jehn, R. The new Space Debris Mitigation (SDM 4.0) long-term evolution code, *Proceedings of the 5th European Conference on Space Debris*, ESA SP-672, CDROM, European Space Agency, Noordwijk, The Netherland, 2009.
11. Liou, J.-C., Johnson, N.L. A sensitivity study of the effectiveness of active debris removal in LEO, *Acta Astronautica*, 64 (2009) 236-243.
12. Bastida Virgili, B., Krag, H. Strategies for active removal in LEO, *Proceedings of the 5th European Conference on Space Debris*, ESA SP-672, CDROM, European Space Agency, Noordwijk, The Netherland, 2009.

13. Liou, J.-C., Johnson, N.L. Controlling the growth of future LEO debris populations with active debris removal, *Acta Astronautica*, 66 (2010) 236-243.
14. Rossi, A., Cordelli, A., Farinella, P., Anselmo, L. Collisional evolution of the Earth's orbital debris cloud, *Journal of Geophysical Research - Planets*, 99 (1994) 23195-23210.
15. Liou, J.-C., Johnson, N.L. Risks in space from orbiting debris, *Science*, 311 (2006) 340-341.
16. Klinkrad, H., Johnson, N.L. Space debris environment remediation concepts, *Proceedings of the 5th European Conference on Space Debris*, ESA SP-672, CDROM, European Space Agency, Noordwijk, The Netherland, 2009.
17. De Luca, L. et al. Active space debris removal by hybrid propulsion module, Research Project Proposal No. 2010BTERWJ to the Italian Ministry of Education, University and Research (MIUR), 2012.
18. De Luca, L. et al. Active space debris removal by hybrid rocket propulsion, *Proceedings of the 2nd European Workshop on Active Debris Removal*, CNES HQ, Paris, France, 2012.
19. Kawamoto, S. Debris environment remediation: Its necessity and target, 30th IADC Plenary Meeting, Montreal, Canada, 2012.
20. Joint Space Operations Center (JSpOC), Space-Track.org, The Source for Space Surveillance Data, [www.space-track.org], USSTRATCOM, 2012.
21. Nishida, S.-I., Kawamoto., S. Strategy for capturing of a tumbling space debris, *Acta Astronautica*, 68 (2011) 113-120.
22. Pinson, R.M. et al. Orbital express advanced video guidance sensor: ground testing, flight 1049 results and comparisons, AIAA Guidance, Navigation and Control Conference and Exhibit, Honolulu, USA, 18-21 Aug 2008.
23. Bodin, P. et al. PRISMA: an in orbit test bed for guidance, navigation, and control experiments, *J. Spacecraft Rockets*, 46 (2009) 615-623.
24. Fasan, G., Accardo, A., Grassi, M. A stereo-vision based system for autonomous navigation of an in-orbit servicing platform. In: *AIAA Infotech@Aero-space 2009*, Seattle, USA, ISBN-10: 1-56347-971-0, April 2009.
25. Gonzalez, R.C., Woods, R.E. *Digital image processing*, 3rd edition, Pearson International, Upper Saddle River, 2008.
26. Alferez, R., Wang, Y.-F. Geometric and illumination invariants for object recognition, *IEEE Transac. Pattern Anal Mach Intell.*, (2009) doi:10.1109/34.771318 1081.
27. Sako, H., Whitehouse, M., Smith, A., Sutherland, A. Real-time facial-feature tracking based on matching techniques and its applications, Pattern Recognition, Vol. 2, *Proceedings of the 12th IAPR International Conference on Computer Vision and Image Processing*, Jerusalem, Israel, October 1994.
28. Burkhardt, H. et al. Evaluation of propulsion systems for satellite end of life de-orbiting, AIAA Paper AIAA-2002-4208, 2002.
29. Patera, R. P., Ailor, W. H., *The Realities of Reentry Disposal*, Center for

Orbital and Reentry Debris Studies, The Aerospace Corporation, Los Angeles.
30. NASA Official Website - http://www.nasa.gov/.
31. Altman, D., *Highlights in Hybrid Rocket Propulsion History*, The 10th International Workshop on Combustion and Propulsion, Lerici – La Spezia, September 2003.
32. Chiaverini, M.J., Kuo, K.K. Fundamentals of hybrid rocket combustion and propulsion, *AIAA Progress in Astronautics and Aeronautics*, Vol. 218, 2007.
33. Marxman, G.A., Gilbert, M., *Turbulent Boundary Layer Combustion in the Hybrid Rocket*, 9th International Symposium on Combustion, The Combustion Institute, 1963.
34. DeLuca, L.T., *Problemi Energetici in Propulsione Aerospaziale*, 1st Edition, Politecnico di Milano, 2007;
35. Sutton, G. P., Biblarz, O., *Rocket Propulsion Elements, 7th Edition*, John Wiley & Sons, 2001.
36. Yuasa, S., Shimada, O., Imamura, T., and Yamamoto, K., "*A Technique for Improving the Performance of Hybrid Rocket Engines*", *35th AIAA/ASME/SAE/ASEE Joint Propulsion Conference and Exhibit*, Los Angeles, California, June 1999, *Paper*. 992322.
37. Tamura, T., Yuasa, S. and Yamamoto, K,*"Effect of Swirling Oxidizer Flow on Fuel Regression Rate of Hybrid Rockets"*, *35th AIAA/ASME/SAE/ASEE Joint Propulsion Conference and Exhibit*, Los Angeles, California, June 1999, *Paper*. 992323.
38. Gibbon, D., Haag, G.S. Investigation of an alternative geometry hybrid rocket for small orbit transfer, SPBB-26287-01, Surrey Satellite Technology Limited, 27 July 2001.
39. Czysz, P.A., Bruno, C. *Future spacecraft propulsion systems: Enabling technologies for space explora-tion*, Springer Praxis, 2006.
40. Ventura, M., Wernimont, E., Heister, S., Yuan, S. Rocket Grade Hydrogen Peroxide (RGHP) for use in propulsion and power devices – Historical discussion of hazards, Paper AIAA-2007-5468, 2007.
41. Encyclopedia Astronautica - http://www.astronautix.com/engines/11d49.htm.